Article

The Release of Grape Pomace Phenolics from Alginate-Based Microbeads During Simulated Digestion In Vitro: The Influence of Coatings and Drying Method

Josipa Martinović , Jasmina Lukinac , Marko Jukić , Rita Ambrus , Mirela Planinić , Gordana Šelo , Gabriela Perković , Ana Bucić-Kojić *

Posted Date: 19 October 2023

doi: 10.20944/preprints202310.1205.v1

Keywords: grape pomace extract; phenolic compounds; encapsulation; drying; microbeads characterization; release in vitro

Article

The Release of Grape Pomace Phenolics from Alginate-Based Microbeads During Simulated Digestion In Vitro: The Influence of Coatings and Drying Method

Josipa Martinović [1], Jasmina Lukinac [1], Marko Jukić [1], Rita Ambrus [2], Mirela Planinić [1], Gordana Šelo [1], Gabriela Perković [1] and Ana Bucić-Kojić [1,*]

[1] Faculty of Food Technology Osijek, Josip Juraj Strossmayer University of Osijek, F. Kuhača 18, HR-31 000 Osijek, Croatia; josipa.grgic@ptfos.hr (J.M.); jasmina.lukinac@ptfos.hr (J.L.); marko.jukic@ptfos.hr (M.J.); mplanini@ptfos.hr (M.P.); gordana.selo@ptfos.hr (G.Š.); gperkovic@ptfos.hr (G.P.)

[2] Faculty of Pharmacy, Institute of Pharmaceutical Technology and Regulatory Affairs, University of Szeged, H-6720 Szeged, Hungary; ambrus.rita@szte.hu

* Correspondence: abucic@ptfos.hr; Tel.: +385-31-224-334

Abstract: Grape pomace is a byproduct of wineries and sustainable source of bioactive phenolic compounds. Encapsulation of phenolics with a well-chosen coating may be a promising means of delivering them to the intestine, where they can then be absorbed and exert their health-promoting properties. Ionic gelation of grape pomace extract with natural coatings (sodium alginate and its combination with maltodextrins, gelatin, chitosan, tragacanth gum, and gum arabic) was performed, and the resulting hydrogel microbeads were then air-, vacuum-, or freeze-dried to prevent their spoilage. The physicochemical characterization (size, shape, texture, and morphology) of the microbeads and the in vitro release of phenols from microbeads were studied and a good relationship between them was established. Freeze-dried microbeads showed the highest cumulative release of phenols as in the intestinal phase (23.31–43.27 mg_{GAE}/g_{MB}), followed by vacuum-dried (23.31–35.41 mg_{GAE}/g_{MB}) and air-dried (22.74–31.38 mg_{GAE}/g_{MB}), while the most suitable release dynamics in the intestinal phase were observed for alginate-based microbeads combined with gelatin (58.4%), gum arabic (34%) and 1.5% *w/v* chitosan (15.3%). The results highlight the importance of developing encapsulated formulations containing a natural source of bioactive compounds that can be used in various functional foods and pharmaceutical products.

Keywords: grape pomace extract; phenolic compounds; encapsulation; release in vitro; drying hydrogel microbeads; microbeads characterization

1. Introduction

In recent years, there has been a growing interest in the encapsulation of bioactive compounds from various natural sources due to their potential health benefits and functional properties [1]. One such source is grape pomace (GP), a byproduct of the wine industry, which is rich in phenolic compounds known for their antioxidant and health-promoting properties [2]. The encapsulation of these phenolic compounds using the ionic gelation method holds a significant promise in enhancing their stability, bioavailability, and controlled release. Ionic gelation is encapsulation method that involves formation of crosslinked hydrogels through the interaction between oppositely charged ions, typically involving a polyanion and cationic material, resulting in the entrapment of active compound(s) within the hydrogel matrix [3]. This method is widely used due to its simplicity and ability to encapsulate a wide range of bioactive compounds making it crucial technique in pharmaceutical and biotechnology applications [4,5]. Hydrogels obtained after ionic gelation are susceptible to spoilage, therefore drying is an important step to ensure their long-term stability and preservation.

 doi:10.20944/preprints202310.1205.v1

There is a constant searching for new coatings and their combinations to obtain natural-polymer-based hydrogels. Choice of coating(s) impact hydrogel characteristics such as geometric parameters, textural properties, morphology, swelling, porosity, and other, which can further affect stability and release of encapsulated active compound. Each of the natural coatings used in this study—sodium alginate, maltodextrin, gums Tragacanth and Arabic, gelatin from cold fish skin, and chitosan—possesses unique properties that can influence the encapsulation and release of phenolic compounds. Sodium alginate, polysaccharide derived from brown algae, is most commonly used in various biomedical fields, including drug delivery [6], wound healing [7], tissue engineering [8], and regenerative medicine [9]. Because its excellent properties such as biocompatibility, gel-forming ability, non-toxicity, and biodegradability [6], sodium alginate is often used for ionic gelation of various compounds. On the other hand, maltodextrin is also commonly used due to its favorable properties including emulsification, water solubility, low viscosity at high concentrations, biodegradability, and film formation [10], but mainly for spray-drying and freeze-drying methods [11]. Maltodextrins have dextrose equivalent (DE) that indicates the degree of hydrolysis or polymerization of starch molecules and affects its functional properties. Therefore, maltodextrins with lower DE values have longer glucose chains and higher molecular weights, impacting solubility, viscosity, and stability [12]. Gum Tragacanth and gum Arabic are both natural exudate gums that have been used as coatings for encapsulation of various compounds [13]. Gum Arabic has been employed for encapsulating grape seed oil [14], turmeric oleoresin [15], and blackberry derived bioactive compound [16], but has been also shown to enhance enzyme and probiotic stability [17,18]. Gum Tragacanth, while primarily researched for rheological properties and structural components, shows potential for antimicrobial and antioxidant applications, though specific biomedical uses are less explored [19]. Fish gelatin has gained attention in various fields, including biomedical application and encapsulation. If offers several advantages over mammalian gelatin, such as economical production using discarded fish byproducts and fewer personal or religious restrictions [20]. Fish gelatin has been explored for its potential in wound dressing and healing, gene therapy, tissue engineering, implants, bone substitutes, and drug delivery systems [21]. Chitosan, a modified biopolymer derived from chitin, has been used various industries, including food, cosmetics, textile, and agriculture [22]. It has been used for encapsulation of many compounds such as flavors, essential oils, vitamins, enzymes, and aroma to protect them from degradation and/or to control their release [22]. In addition to its encapsulation properties, chitosan coatings have shown antibacterial activity making them suitable for pharmaceutical and biomedical applications [23]. It has been utilized for wound dressing [24], drug delivery [25], and tissue engineering [26]. Overall, the choice of coating material has a significant impact in the encapsulation process on encapsulation efficiency, physicochemical characteristics of produced particles and further use.

In this study, phenol-rich Cabernet Sauvignon grape pomace extract (CSE) was encapsulated by ionic gelation method using alginate-based blends with maltodextrins, gums Tragacanth and Arabic, cold fish skin gelatin and chitosan, followed by three drying methods—air, vacuum, and freeze drying. Influence of these blends and drying methods on size and shape parameters, texture, morphology, and finally in vitro release of phenolic compounds was investigated. This research plays a crucial role in advancing the understanding of the release of phenolic compounds, highlighting its significance in the fields of controlled release, bioavailability, and targeted delivery of not only phenolic compounds but also other active ingredients encapsulated in natural-polymer-based systems.

2. Results and Discussion

2.1. Encapsulation Efficiency of the Total Phenolic Compounds

The efficiency of encapsulation (*EE*) of phenol-rich grape pomace extract (CSE) in various alginate-based blends was assessed, showing the potential to improve *EE* by introducing various natural coatings in addition to sodium alginate.

In Figure 1, the data illustrate that using sodium alginate (SA) alone resulted in the lowest *EE* at 36.54%.

Preprints (www.preprints.org) | NOT PEER-REVIEWED | Posted: 19 October 2023 doi:10.20944/preprints202310.1205.v1

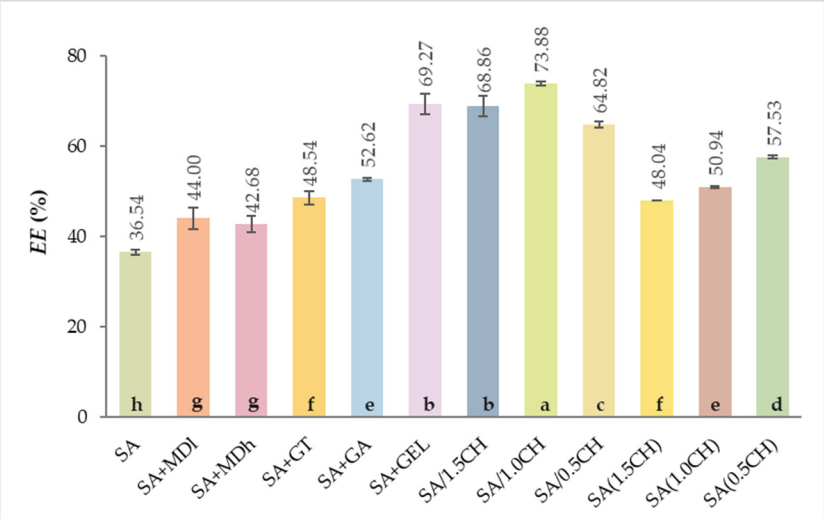

Figure 1. Encapsulation efficiency (*EE*, %) of phenol-rich grape pomace extracts using various coatings (SA—sodium alginate, and combinations of sodium alginate: with maltodextrin (dextrose equivalent 4–7)—SA+MDl, maltodextrin (dextrose equivalent 16.5–19.5)—SA+MDh, gum Tragacanth—SA+GT, gum Arabica—SA+GA, gelatin—SA+GEL; with chitosan (CH) dispersed in crosslinking solution at various concentrations: SA/1.5CH—1.5% (w/v), SA/1.0CH—1.0% (w/v), SA/0.5CH—0.5% (w/v); and with CH when alginate hydrogels were immersed in CH solution of various concentrations: SA(1.5CH)—1.5% (w/v), SA(1.0CH)—1.0% (w/v), SA(0.5CH)—0.5% (w/v)). Different letters represent significant differences (ANOVA, Duncan's test at $p < 0.05$).

When maltodextrins were combined with SA, *EE* was statistically significantly increased (ANOVA, $p < 0.05$) and was 44.00% and 42.86% for maltodextrin with lower dextrose equivalent, DE 4–7 (SA+MDl) and those with higher dextrose equivalent, DE 16.5–19.5 (SA+MDh), respectively. However, the results of *EE*, obtained with the two maltodextrins used, were not statistically significantly different from each other, although a slightly better result was obtained with the maltodextrin that had a lower DE. Lower DE maltodextrin indicates less hydrolysis and larger molecules creating an effective matrix for phenolic compound encapsulation as found in Laine et al. [27] and also when combined with sodium alginate as seen in Figure 1.

The use of blend of SA with gum Tragacanth (SA+GT) and gum Arabic (SA+GA) resulted in further improvement of *EE*, reaching 48.54% and 52.62%, respectively (Figure 1). It is known from the literature that the concentration and the coating ratio play an important role in the encapsulation process. Apoorva et al. [28] investigated the influence of different ratios (100:0, 67:33, 50:50, 33:67) of 2% (w/v) SA and 2% (w/v) GT on the *EE* of phenolic compounds extracted from *Basella* species using the ionic gelation method. The obtained *EE* values ranged from 70% to 82%, and with an increase in the alginate content increase of *EE* was proportionally seen. The *EE* obtained with SA+GA was comparable to those found in the literature. In their study, Li et al. [29] encapsulated tea polyphenols with 2 wt% SA and 2 wt% GA in a ratio of 80:20, resulting in *EE* of 48.56%. Other than concentration used, the structure of the coatings also plays a role in the encapsulation process. GT is mainly composed of branched polysaccharides, while GA is a complex mixture of polysaccharides, glycoproteins, and other compounds with a highly branched structure [30]. The structure of GA and its functional groups promote favorable interactions with phenolic compounds [31] and retain them in the hydrogel. Similar interactions with phenolic compounds form proteins such as gelatin (GEL) through various types of bonding, including hydrogen bonding, electrostatic interactions, and hydrophobic interactions [32], improving *EE*. As shown in Figure 1, the addition of GEL to SA (SA+GEL) led to an enhancement in *EE* (69.27%).

When chitosan (CH) was combined with SA and dispersed in the crosslinking solution $CaCl_2$ at three concentrations (1.5%—SA/1.5CH, 1.0%—SA/1.0CH, and 0.5%—SA/0.5CH), the percentage of *EE* ranged from 64.82% to 73.88%, with SA/1.0CH being the highest *EE* compared to all prepared mixtures (Figure 1). In this way, the chitosan is immediately incorporated into the hydrogel matrix

 doi:10.20944/preprints202310.1205.v1

during encapsulation and can therefore be more evenly distributed in the hydrogel. When alginate hydrogels were immersed in CH at three concentrations (1.5%—SA(1.5CH), 1.0%—SA(1.0CH), 0.5%—SA(0.5CH)), *EE* was lower than the previous case and ranged from 48.04% to 57.53% (Figure 1). Overall, chitosan has a positive charge due to the amino groups, while phenolic compounds often have a negative charge, and this electrostatic attraction can improve *EE* [33].

2.2. Hydrogel Microbeads and Dried Microbeads Characterization

2.2.1. Size, Shape, and Morphology

After CSE encapsulation, the hydrogel microbeads were stabilized by drying using three methods: air drying, vacuum drying, and freeze drying to prevent their spoilage, resulting in three different types of dried microbead. The hydrogel microbeads and the dried microbeads were characterized on the basis of their geometrical properties, especially size and shape parameters, while the morphology of the dry microbeads was evaluated using scanning electron microscope (SEM), since the above parameters are important for understanding the release of the active ingredient from the microbeads into the digestive tract. The effect of drying method and coating on the ability to release phenolic compounds from dried microbeads in digestive juices was monitored in vitro.

The results of the analysis of the size and shape parameters presented in the attached materials (Tables S1–S4 and Tables S5–S7) show that the coatings used have an influence on the studied size and shape parameters of the hydrogel microbeads. For the dried microbeads, the size and shape parameters were influenced by the coatings used and the drying process individually or in interaction, as each drying method in combination with the individual coating(s) had a different influence on the size and shape parameters studied.

Considering only the hydrogel microbeads, it can be seen that the smallest microbeads were obtained with only one coating for CSE encapsulation, i.e., SA, where the average surface area of a particle was 11.84 mm^2 (Table S1), the perimeter was 13.21 mm (Table S2), and the maximum and minimum Feret were 4.24 mm and 3.65 mm, respectively (Tables S3 and S4). The addition of the subsequent coating to SA affected the enlargement of the hydrogel microbeads, with the largest microbeads formed when the SA/1.5CH coating was used. These particles had a projected area of 19.32 mm^2 (Table S1), perimeter of 17.91 mm (Table S2), a maximum Feret of 6.65 mm (Table S3), and a minimum Feret of 3.89 mm (Table S4).

As expected, drying removed some of the moisture from the hydrogel microbeads, resulting in a significant reduction in size for all dried microbeads. In general, the microbeads showed the least changes in size parameters after freeze-drying, while the largest changes were observed in the air-dried microbeads compared to the hydrogel microbeads. More specifically, the area reduction (Table S1) of the microbeads after freeze-drying compared with hydrogel microbeads ranged from 31% (SA+GA) to 62% (SA), which was statistically less significant ($p < 0.05$) than the area reduction after vacuum drying, which ranged from 80% (SA+MDl, SA+GEL) to 88% (SA(0.5CH)), and after air drying, where the area reduction ranged from 83% (SA+MDl, SA+GEL) to 89% (SA(1.5CH), SA(1.0CH)). A similar trend is observed in the reduction of the perimeter of the dried microbeads compared with the hydrogel microbeads (Table S2), where the smallest change in the perimeter of the microbeads after freeze-drying ranged from 7% (SA+GA) to 35% (SA), more significant changes in the perimeter were then observed after vacuum drying, ranging from 53% (SA+MDl) to 67% (SA(0.5CH)), and the largest decrease in perimeter was observed after air drying, ranging from 59% (SA+GT) to 67% (SA (1.5CH), SA(1.0CH)). The $Feret_{MAX}$ values presented in Table S3 show that the highest value was attributed to SA/1.5CH dried microbeads, regardless of the drying method employed. After the drying process, the SA+GEL microbeads consistently exhibited the highest $Feret_{MIN}$ values across all drying methods (Table S4).

As mentioned above, the drying process and the coating(s) used, as well as their interactions, had a statistically significant ($p < 0.05$) influence on the shape parameters, circularity, roundness, and solidity, of the dried microbeads, while the coating used influenced the tested shape parameters of the hydrogel microbeads. Table S5 presents the circularity results for both hydrogel microbeads and

 doi:10.20944/preprints202310.1205.v1

dry microbeads, quantifying the degree of conformity to a perfect circle, with values ranging from 0 to 1, where 1 represents a perfect circular shape. Hydrogel and air-dried microbeads had the least deviation from the regular shape of a circle, with a range of values for circularity of 0.76 (SA/1.5CH) to 0.88 (SA(1.0CH), SA(0.5CH)) for hydrogel microbeads and for air-dried microbeads from 0.74 (SA/1.5CH, SA/0.5CH) to 0.89 (SA(0.5CH)). Vacuum-dried microbeads had a smaller circularity value (0.68–0.89), while freeze-dried microbeads had the largest deviation from the shape of a circle with circularity ranging from 0.63 (SA/1.5CH) to 0.78 (SA+MDl).

Roundness, which quantifies the curvature of the edges and corners of hydrogel microbeads and dried microbeads, is detailed in Table S6. Across all three drying methods, the roundness of dried microbeads generally decreased compared with hydrogel microbeads. The roundness of the hydrogel microbeads ranged from 0.59 to 0.91, and that of the air-dried microbeads ranged from 0.56 to 0.88, while the greatest deviation in roundness values from the hydrogels was observed for the microbeads obtained by vacuum drying and freeze-drying, which ranged from 0.52 to 0.89 (Table S6).

Table S7 presents the solidity values of the examined samples. Solidity is a shape parameter that serves as an indicator of particle compactness and smoothness, with values falling within the range of 0 to 1, where 1 signifies a highly compact particle. For the hydrogel microbeads, the solidity values ranged from 0.97 to 0.98 (Table S7). However, after the drying process, these values decreased, indicating a deviation from the regular shapes and the presence of voids in the samples. Nevertheless, after drying, the solidity values remained in the range of 0.92 to 0.97, but there was a statistically significant difference ($p < 0.05$) compared to the hydrogels, with a greater deviation observed in the vacuum- dried and freeze-dried microbeads than in the air-dried microbeads (Table S7). It is important to note that solidity exclusively pertains to the edges and borders of both hydrogel and dried microbeads, therefore a more detailed examination of microbead morphology was performed using SEM.

In general, considering all the shape parameters determined (Tables S5–S7), it can be concluded that when CSE was encapsulated with combination of SA and CH dispersed in crosslinking solution, the microbeads (hydrogel and dried) exhibited the most irregular shape, with the irregularity of the particles increasing with increasing CH concentration.

Morphology of dried microbeads investigated by SEM is shown in Supplementary Materials (Figure S1), whereas morphology of microbeads (SA+GT), (SA/1.5CH), and (SA(1.5CH)–SA(0.5CH)) are shown in following paragraphs.

Air-dried microbeads exhibited surface furrows and cracks (Figure 2A), although these features were less pronounced following vacuum drying (Figure 2B). In the case of freeze-dried microbeads, surface depressions were observed, however, higher magnification revealed the absence of cracks (Figure 2C).

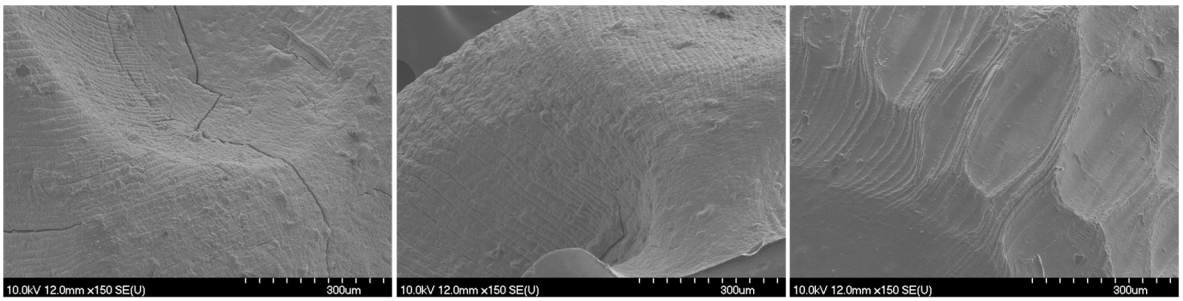

A (i) B (i) C (i)

Preprints (www.preprints.org) | NOT PEER-REVIEWED | Posted: 19 October 2023 doi:10.20944/preprints202310.1205.v1

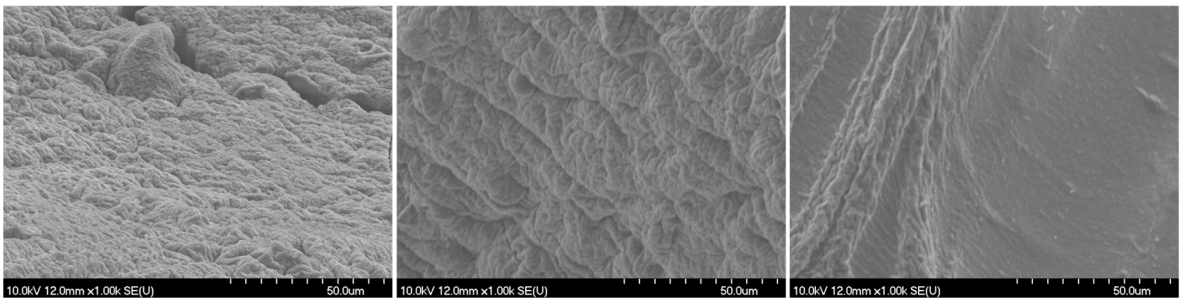

A (ii) B (ii) C (ii)

Figure 2. SEM image of (**A**) air-dried microbeads, (**B**) vacuum-dried microbeads and (**C**) freeze-dried microbead of grape pomace extract encapsulated with a combination of sodium alginate and Tragacanth gum as a coating (SA+GT); and their outer layer with the scale bar of 300 μm (**i**) and 50 μm (**ii**).

Air drying often leads to uneven drying, resulting in the formation of cracks, deformations, or inconsistencies in particle size and shape, which can be troublesome when uniformity is crucial. Hydrogels are also prone to shrinkage and distortion during air drying due to the gradual evaporation of water, which typically starts at the outer layers and progresses inward [34]. The SEM images offer insights into the morphology of the SA/1.5CH microbeads, revealing their distinct characteristics. Notably, the air-dried microbeads exhibit a deformed structure, as evidenced in Figure 3A, while those subjected to vacuum drying display a prominent ellipsoidal shape, as evident in Figure 3B. These observations corroborate the circularity and roundness parameters measured (Tables S5 and S6). Furthermore, at the same magnification and size scale, air- and vacuum-dried microbeads can be seen whole on SEM images, while freeze-dried ones cannot (Figure 3C). This confirms the differences in size parameters area and perimeter found for SA/1.5CH microbeads (Tables S1 and S2). Similar case was noticed for SA/1.0CH microbeads, where 1.0% (w/v) chitosan was dispersed in $CaCl_2$ (see Supplementary Materials Figure S1).

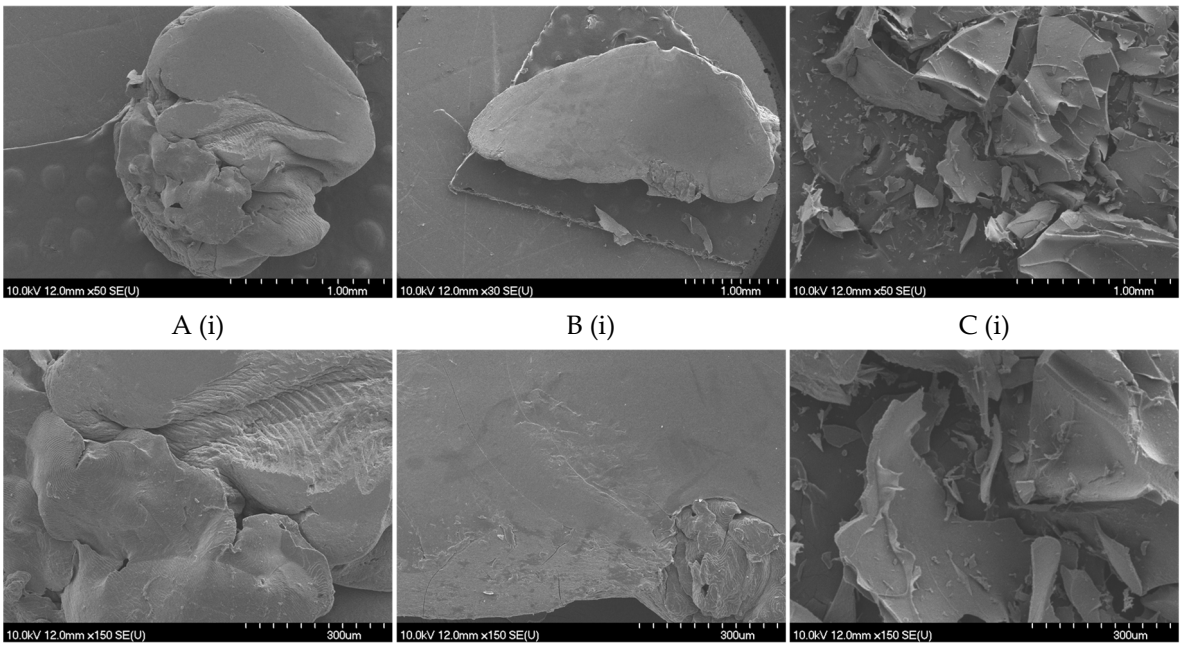

A (i) B (i) C (i)

A (ii) B (ii) C (ii)

Figure 3. SEM image of (**A**) air-dried microbeads, (**B**) vacuum-dried microbeads and (**C**) freeze-dried microbead of grape pomace extract encapsulated with a combination of sodium alginate and 1.5% (w/v) chitosan dispersed in calcium chloride (SA/1.5CH); and their outer layer with the scale bar of 1 mm (**i**) and 300 μm (**ii**).

Preprints (www.preprints.org) | NOT PEER-REVIEWED | Posted: 19 October 2023 doi:10.20944/preprints202310.1205.v1

Freeze dried SA(1.5CH) and SA(1.0CH) microbeads exhibited a smooth surface with minimal folds and a distinctive teardrop-like shape (Figure 4A,B), while SA(0.5CH) microbeads did not adopt a similar shape but maintained a smooth surface (Figure 4C).

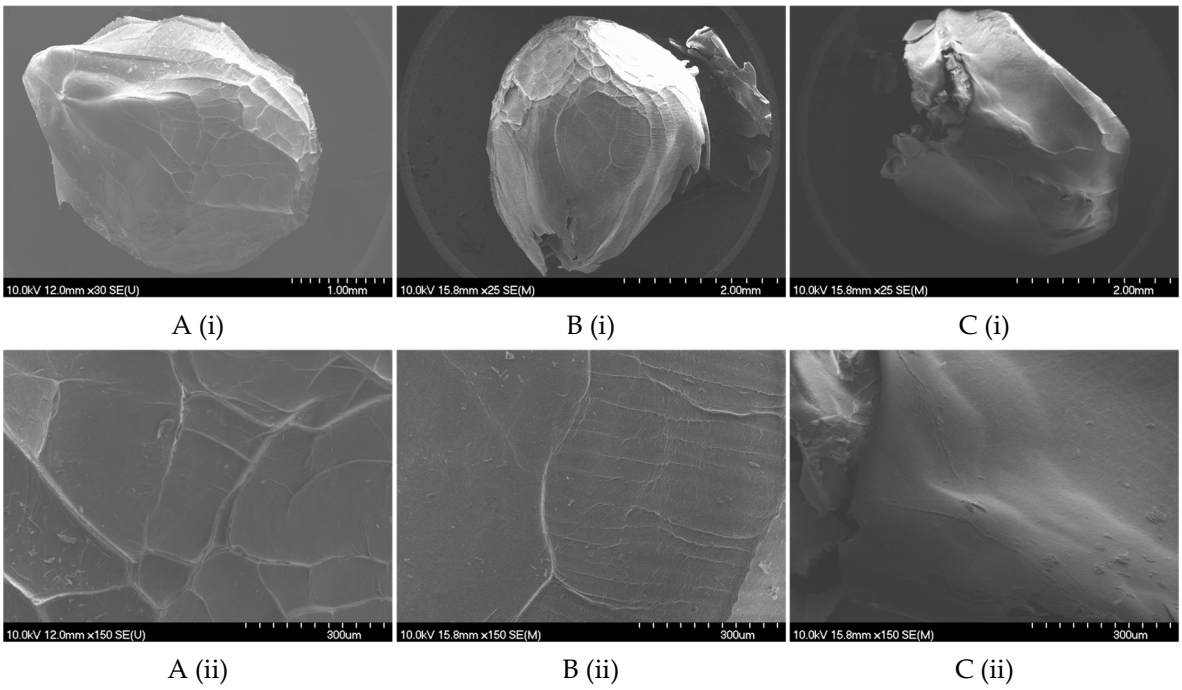

Figure 4. SEM image of freeze-dried microbead of grape pomace extract encapsulated with a combination of sodium alginate and (**A**)—1.5% (w/v) chitosan (SA(1.5CH)), (**B**)—1.0% (w/v) chitosan (SA(1.5CH)), and (**C**) 0.5% (w/v) chitosan (SA(0.5CH)) in immersion solution; and their outer layer with the scale bar of 1 mm and 2 mm (**i**) and 300 μm (**ii**).

Figures 3 and 4 illustrate the significant influence of employing identical coatings on microbead morphology and geometrical characteristics, while emphasizing the impact of CH concentration as well. Additionally, freeze-drying has notable advantages for maintaining geometric parameters and morphology of microbeads compared to air and vacuum drying, because water is sublimated slowly from the frozen state. While dried microbeads maintain their initial contours, it is worth noting that surface imperfections such as dents, may arise [34] as seen in SEM images displayed in Supplementary Materials (Figure S1). Nonetheless, this conservation of the original structure allows freeze-dried microbeads to closely mimic the characteristics of hydrogel microbeads.

2.2.2. Texture

The texture parameter, hardness, of both hydrogel microbeads and dried microbeads was evaluated, and the results are shown in Table S8.

The results show that different coatings and drying methods have an impact on the hardness of hydrogel microbeads. Bušić et al. [35] performed encapsulation of dandelion polyphenols in alginate hydrogels coupled with whey protein isolate, cocoa powder, or carob as additional coatings, and their results showed increased strength compared to pure alginate hydrogels. In this study, the SA+MDh hydrogel microbeads had the highest measured hardness (0.44 N), but this was not statistically significantly different from the SA+GEL, SA/1.5CH, SA/0.5CH, and SA(0.5CH).

In addition, air drying and vacuum drying significantly increased the hardness of the microbeads compared to the hydrogel microbeads, as shown in the results presented in Table S8. Hydrogel microbeads can retain large amounts of liquid due to their hydrophilicity [36]. Therefore, the increase in hardness can be attributed to the removal of water content during the drying process, resulting in the dried microbeads having a more compact structure that requires greater force for compression.

 doi:10.20944/preprints202310.1205.v1

When comparing the dried microbeads, a different effect of the drying method on hardness was found. Vacuum drying resulted in greater changes in microbead hardness, with the SA(0.5CH) microbeads having the highest value. On the other hand, freeze-drying had a lesser effect on hardness compared to hydrogel microbeads, with SA microbeads having the highest hardness of 3.40 N.

2.3. In Vitro Release of Encapsulated Phenolic Compounds

Considering that the potential site of absorption of phenolic compounds is the intestinal phase, the increase of total phenolic compounds (TPC) release in the intestinal phase (IP) was a more important criterion for the selection of a suitable coating and drying method of hydrogel microbeads. Results obtained in this study showed that the coatings and drying methods used affect the release of TPC from the dried microbeads.

The concentration profile of cumulative release of TPC from air-dried, vacuum-dried, and freeze-dried microbeads prepared with 12 coatings was evaluated for the oral (OP), gastric (GP), and IP phases of simulation digestion in vitro without digestive enzymes (Figures S2–S5). In general, a similar trend of increasing TPC release was observed through three digestion phases, regardless of the type of drying of the hydrogel microbeads although the highest cumulative release was observed in IP during for freeze-dried (23.65-43.27 mg_{GAE}/g_{MB}), followed by vacuum-dried (23.31-35.41 mg_{GAE}/g_{MB}) and finally air-dried (22.74-31.38 mg_{GAE}/g_{MB}) microbeads.

Freeze-drying is a widely used method to preserve phenolic compounds after ionic gelation because the structure of the microbeads is preserved (Figure S1) and the surface area is increased by removing ice crystals, creating dents that promote faster diffusion of phenolic compounds. Abdin et al. [37] found similar results, with higher release of TPC from freeze-dried microbeads compared to vacuum-dried ones. Air drying exposes hydrogel microbeads to humidity, light, and temperature fluctuations, which can lead to their decomposition and thus unstable and unpredictable release (Figures S2–S5). Air-dried microbeads were the smallest (Tables S1–S4) and had the highest hardness (Table S8). Their dense structure hinders the penetration of digestive fluids, which reduces the release of phenolic compounds, similar to the results published by Guzman-Villanueva et al. [38]. In addition, air-dried microbeads showed the lowest deviation from sphericity (Tables S5 and S6) (Figure S1), implying that the contact area with digestive fluids is smaller, resulting in a lower concentration of released TPC. Vacuum drying is gentler than air drying and has a favorable effect on the stability of phenolic compounds [39]. The advantage over air drying is the controlled drying conditions, which results in a product of more uniform quality. Compared with air-dried microbeads, vacuum-dried microbeads had slightly larger size parameters (Tables S1–S4), higher deviation from the circle (Tables S5 and S6) (Figure S1), and lower hardness (Table S8), resulting in a similar release pattern but with a slightly higher content of released TPC (Figures S2–S5).

It was also found that the coatings used had different effects on the release of phenolic compounds, and the highest cumulative content of TPC in the IP was observed when using CH dispersed in $CaCl_2$ (40.78-43.27 mg_{GAE}/g_{MB}), followed by CH, when it was used as an immersion solution for hydrogel microbeads (35.47-36.86 mg_{GAE}/g_{MB}), and then GT (31.02 mg_{GAE}/g_{MB}), GA (29.77 mg_{GAE}/g_{MB}), GEL (28.05 mg_{GAE}/g_{MB}), SA (27.7 mg_{GAE}/g_{MB}), MDh (24.50 mg_{GAE}/g_{MB}), and MDl (23.65 mg_{GAE}/g_{MB}). The results show that SA, as one of the most commonly used coatings to protect bioactive substances, has lower cumulative content in IP compared to most of the tested coatings, except when combined with maltodextrins. Bušić et al. [35] found that SA microbeads have a porous structure and tend to release their contents quickly, and it is also visible in this study on the Figure S1. Furthermore, since SA microbeads are porous and not stable enough in the low pH gastric environment encapsulated compounds are faster released [40], and so there is justification for applying an additional coating to improve effect a more controlled release of TP and its delivery into the IP.

The percentage of cumulative TPC release in the three digestion phases for the tested coatings is shown in Figure 5A–C.

Preprints (www.preprints.org) | NOT PEER-REVIEWED | Posted: 19 October 2023 doi:10.20944/preprints202310.1205.v1

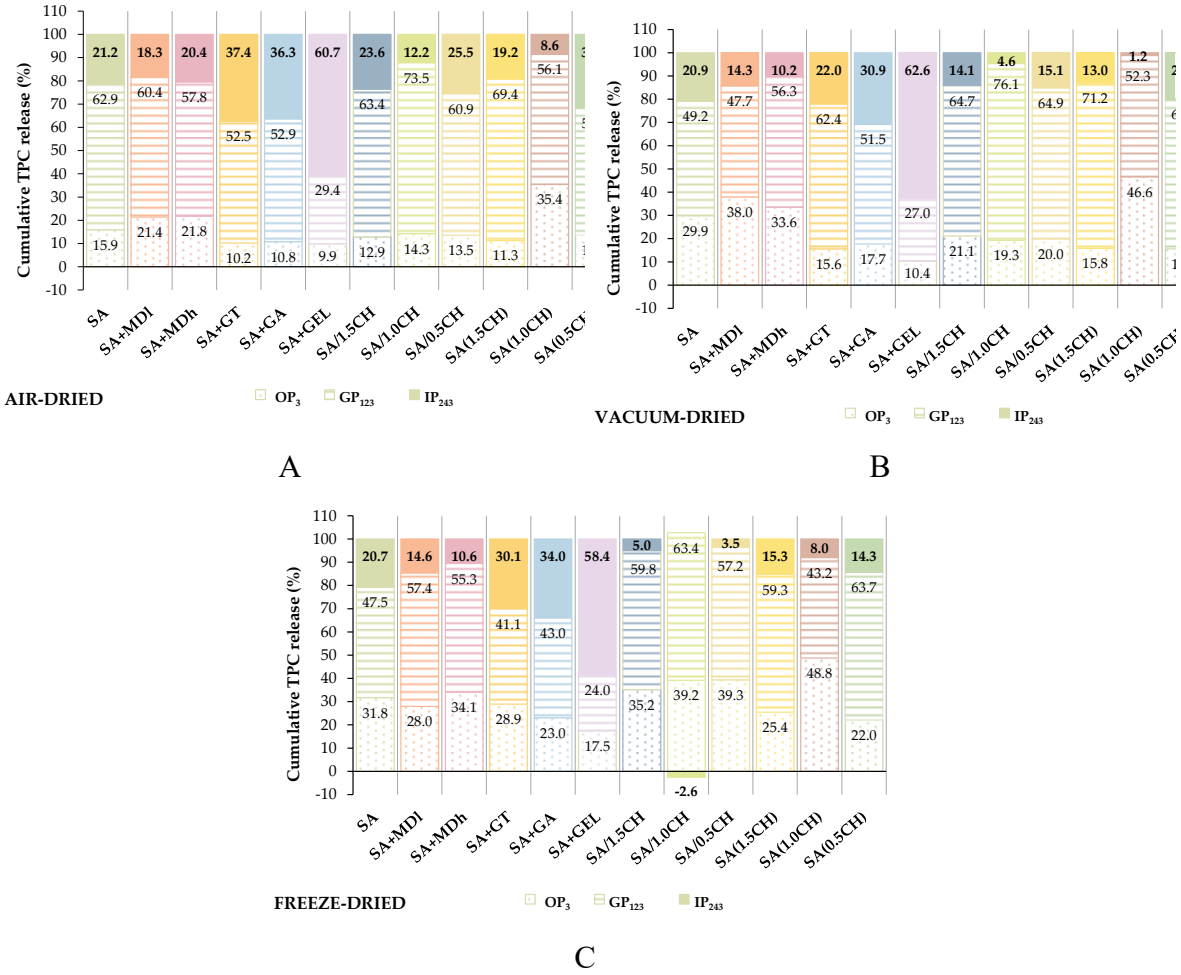

Figure 5. The percentage of cumulative TPC release for each gastrointestinal phase: OP-oral phase, GP-gastric phase, IP-intestinal phase for air-dried (**A**), vacuum-dried (**B**) and freeze-dried (**C**) microbeads (SA—sodium alginate, and combinations of sodium alginate with maltodextrin (dextrose equivalent 4–7)—SA+MDl, maltodextrin (dextrose equivalent 16.5–19.5)—SA+MDh, gum Arabica—SA+GA, gelatin—SA+GEL; with chitosan (CH) dispersed in crosslinking solution at various concentrations: SA/1.5CH—1.5% (w/v), SA/1.0CH—1.0% (w/v), SA/0.5CH—0.5% (w/v); and with CH when alginate hydrogels were immersed in CH solution (image of freeze-dried microbeads presented in manuscript) of various concentrations: SA(1.5CH)—1.5% (w/v), SA(1.0CH)—1.0% (w/v), SA(0.5CH)—0.5% (w/v).

These data indicate the percentage of TPC released in each phase relative to the total percentage of TPC released during the 243-minute digestion. The highest cumulative release of TPC (58.4-62.6%) during IP and lowest value during GP (24-29.4%) and OP (9.9-17.5%) (Figure 5A–C) which is the most desirable TPC release profile (Figure S3E) was observed for SA+GEL microbeads, regardless of the drying method used. This may be related to the fact that the microbeads swell better at intestinal pH, which allows lower diffusion of TPC in the GP and higher in the IP as found by Devi et al. [41].

Further, SA+GT and SA+GA release similar percentage of TPC in IP of 22-37.4% and 30.9-36.3% respectively. Their better TPC release compared to SA at intestinal pH may be attributed to the electrostatic repulsion between the negatively charged carboxyl groups in SA, GA, and GT which promotes greater microbeads swelling [28,42]. Tsai et al. [43] also observed increased release of phenolic compounds in IP when they encapsulated radish by-product juice with a SA+GA coating combination compared with SA. Similarly, Apoorva et al. [28] reported an increased release of phenolic compounds extracted from *Basella* species when a combination of SA+GT was used.

 doi:10.20944/preprints202310.1205.v1

Generally, when CH applied, it was found that SA/1.0CH and SA(1.0CH) microbeads exhibited the least desirable release dynamics regardless of drying method (Figure 5A–C). Figure 5C even shows a negative cumulative percentage (-2.65%) of TPC release in the IP phase for SA(1.0CH) microbeads. On the other hand, considering that freeze-drying was shown to be the best method in terms of TPC release (Figures S2–S5), it can be concluded that among all tested microbeads prepared with CH, the highest percentage of TPC was released in IP from SA(1.5 CH) microbeads (15.3%) (Figure 5C). A similar conclusion was reached by Dai et al. [44] when they studied the effects of these two methods of addition CH on the release of nifedipine. They observed a better release profile of microbeads immersed in a 0.1% (w/v) CH solution than when CH dispersed in a $CaCl_2$ solution because the microbeads swell more in the higher pH range due to less bonding between the carboxyl groups of the alginate and the amino groups of CH [44].

When chitosan is added to the crosslinking solution and becomes an integral part of the hydrogel network, it can interact with the phenolic compounds via hydrogen bonding and electrostatic interactions [45]. However, extensive optimization may be required to obtain a specific release profile, as the distribution of chitosan in the hydrogels may not be uniform and may lead to variations in the release rate. On the other hand, when hydrogel microbeads are immersed in chitosan after formation, the primary interaction between chitosan and hydrogel occurs at the surface, resulting in a lower concentration of chitosan in the bulk of the hydrogel [46]. The sustained release of phenolic compounds from the bulk of the microbeads tends to be slower due to the limited penetration of chitosan into the deeper layers of the hydrogel matrix [47,48]. Belščak-Cvitanović at al. [49,50] also observed comparable outcomes, where chitosan coating prolonged the release of green tea phenolic compounds and caffeine from alginate microbeads.

The percentage of cumulative release in IP of MDl microbeads (14.3-18.6%) and MDh microbeads (10.2-20.4%) was lower than that of SA microbeads (20.7-21.2%) regardless of the drying method (Figure 5A–C). It can be assumed that due to a higher percentage of TPC release in OP from MD (21.4%-38% for MDl and 21.8-34.1% for MDh) than from SA microbeads (15.9-31.8%) there is a decrease in the cumulative TPC content in IP (Figure S3A,B). Although results of this study indicate the similar pattern of TPC release for both tested MD, generally MDh contain more reducing sugar groups, thereby expediting phenolic compound release. MDh are more likely to form stable complexes with phenolic compounds, but the formed hydrogels degrade faster, enabling rapid release. Maltodextrins, generally, exhibit excellent chemical stability across a wide pH rang, rendering them suitable for various food and pharmaceutical applications [51].

In the overall view of all the results of this comprehensive investigation, SA+GEL, SA +GA, SA and SA(1.5CH) were found to be the best coatings in terms of release of phenolic compounds in the IP phase. The aforementioned coatings were further used to describe the release kinetics with mathematical models and to evaluate the bioaccessibility of the phenolic compounds, and the results were published in two scientific papers [52,53].

3. Conclusions

Encapsulation of phenol-rich grape pomace extract was performed with twelve coatings based on natural alginate. The encapsulation efficiency was increased for 1.20–2.0-fold when a second coating was added to the sodium alginate, and the highest encapsulation efficiency was obtained when 1.0% (w/v) chitosan was dispersed in the crosslinking solution, resulting in an encapsulation efficiency of 73.88%. However, this does not necessarily mean that the coating that achieves the best encapsulation efficiency also ensures the most desirable release dynamics of TPC in the IP phase in the digestive tract, where it can potentially be absorbed. This is due to the properties of the coatings and their different behavior in the digestive tract depending on pH, ionic strength, interactions, etc.

Subsequently, the obtained hydrogels were subjected to air, vacuum and freeze drying. Analysis of the size, shape, texture, and morphology of the dried microbeads revealed significant differences between the coatings and the drying methods used. These results shed light on the crucial influence of the drying process on the geometrical properties and morphology of the microbeads and, consequently, on the release profiles of the phenolic compounds for specific applications requiring sustained or

 doi:10.20944/preprints202310.1205.v1

controlled release. In addition, the observed differences in the size and shape properties of the microbeads were correlated with the release profiles of the total phenolic compounds during the simulated digestion process, and freeze-drying was found to be the most suitable drying method. Further analysis revealed that sodium alginate and its combination with gelatin, gum arabic, and chitosan at a concentration of 1.5% *w/v* when immersing method used to prepare the microbeads were the most suitable coatings for the release of phenolic compounds during simulated digestion in vitro.

This research demonstrates the critical role of the drying methods and coatings used on the properties of the microbeads and consequently on the bioavailability and bioaccessibility of phenolic compounds, which has valuable implications for further applications in the food and pharmaceutical industries.

4. Materials and Methods

4.1. Reagents and Chemicals

The coatings used were alginic acid sodium salt (SA) from brown algae (low viscosity), gelatin (GEL) from cold water fish skin, gum Arabic (powder) (GA), medium molecular weight chitosan (deacetylated chitin) (CH), gum Tragacanth (GT), maltodextrin (DE 4 -7) (MDl), maltodextrin (DE 16.5–19.5) (MDh), and standard gallic acid monohydrate (98+% A. C. S. reagent) were purchased from Sigma Aldrich (Saint Louis, MO, USA). Folin and Ciocalteu's phenol reagent was purchased from CPA chem (Bogomilovo, Bulgaria), 96% ethanol (p.a.) from Lab Expert (Shenzhen, Guangdong, China), and glacial acetic acid (99.5%) was purchased from Macron Fine Chemicals (Gliwice, Poland). The salts used to prepare the electrolyte solutions were purchased from Acros Organics (Geel, Belgium), Gram Mol (Zagreb, Croatia), and Kemika (Zagreb, Croatia).

4.2. Grape Pomace

Pomace of Cabernet Sauvignon (*Vitis vinifera* L.) variety grape (CS) left after vinification was obtained from Erdut winery (Erdut, Croatia, 2018 harvest). It consisted of grape skins, seeds, and pulp. The pomace was air dried (48 h, 25–27 °C) to reduce the moisture content from 48.60% to 8.41% and stored at room temperature. Before use, the grape pomace was ground to a particle size of up to 1 mm using an ultracentrifugal mill (Retsch ZM200, Haan, Germany).

4.3. Phenol-Rich Grape Pomace Extract Preparation

Phenolic compound extraction from CS was performed in a shaking water bath (Julabo, SW-23, Germany) at 80 °C and 200 rpm for 120 min, using a 50% aqueous ethanol solution as solvent with a grape pomace-solvent ratio of 40 mL/g. After extraction, samples were centrifuged at 11,000 ×*g* for 10 minutes (Z 326 K, Hermle Labortechnik GmbH, Germany). The resulting liquid phenol-rich extract was concentrated to dryness in rotary evaporator at 48 mbar and 50 °C (Büchi, R-210, Flawil, Germany) and that dry extract (CSE) was used for encapsulation.

4.4. Determination of Total Phenolic Content

Total phenolic content (TPC) was determined using the Folin–Ciocalteu method described by Waterhouse [54], with some modifications. Briefly, 3160 µL of distilled water was mixed with 40 µL of sample and 200 µL of Folin–Ciocalteu reagent. After an 8-min incubation period, 600 µL of 20% (w/v) sodium carbonate was added, and the mixture was further incubated at 40 °C. After 30 minutes absorbance was measured at 765 nm against a blank containing distilled water instead of the sample. The results were expressed as gallic acid equivalents (GAE) per g of sample used (extract or microbeads).

4.5. Encapsulation by Ionic Gelation

The prepared CSE (1.0 g) was dissolved in 30% aqueous ethanol solution (20.8 mL) and distilled water (79.2 mL) through continuous mixing on a magnetic stirrer for 180 minutes. To eliminate any

 doi:10.20944/preprints202310.1205.v1

undissolved extract particles, the mixture underwent centrifugation at 15,000 ×*g* for 5 min, after which clear supernatant (90 mL) was separated and used for encapsulation. The rest of the supernatant was used for the determination of TPC.

Twelve different types of hydrogel microbeads were prepared by ionic gelation with a total of 7 different coatings (Table 1).

In all 12 types of hydrogel microbeads, SA was used as the primary coating, whereas the secondary coating (MDl, MDh, GT, GA, GEL or CH) was added to the encapsulation liquid (experimental set #: 2–6), i.e., in crosslinking solution (experimental set #: 7–9) or immersion solution (experimental set #: 10–12).

Table 1. Coatings used for encapsulation.

#	Coating	**Encapsulation feed**		**Crosslinking solution**		**Immersion solution**	
1	**SA**	CSE sodium alginate	1.0% 3.0%	$CaCl_2$	0.25 M	-	
2	**SA+MDl**	CSE sodium alginate maltodextrin (DE 4–7)	1.0% 3.0% 1.2%	$CaCl_2$	0.25 M	-	
3	**SA+MDh**	CSE sodium alginate maltodextrin (DE 16.5–19.5)	1.0% 3.0% 1.2%	$CaCl_2$	0.25 M	-	
4	**SA+GT**	CSE sodium alginate gum Tragacanth	1.0% 3.0% 0.15%	$CaCl_2$	0.25 M	-	
5	**SA+GA**	CSE sodium alginate gum Arabic	1.0% 3.0% 1.6%	$CaCl_2$	0.25 M	-	
6	**SA+GEL**	CSE sodium alginate gelatin	1.0% 3.0% 5.0%	$CaCl_2$	0.25 M	-	
7	**SA/1.5CH**	CSE sodium alginate	1.0% 3.0%	$CaCl_2$ chitosan	0.25 M 1.5%	-	
8	**SA/1.0CH**	CSE sodium alginate	1.0% 3.0%	$CaCl_2$ chitosan	0.25 M 1.0%	-	
9	**SA/0.5CH**	CSE sodium alginate	1.0% 3.0%	$CaCl_2$ chitosan	0.25 M 0.5%	-	
10	**SA(1.5CH)**	CSE sodium alginate	1.0% 3.0%	$CaCl_2$	0.25 M	chitosan	1.5%
11	**SA(1.0CH)**	CSE sodium alginate	1.0% 3.0%	$CaCl_2$	0.25 M	chitosan	1.0%
12	**SA(0.5CH)**	CSE sodium alginate	1.0% 3.0%	$CaCl_2$	0.25 M	chitosan	0.5%

Ionic gelation was performed using a Büchi B-390 encapsulator (Flawil, Switzerland). A 450 µm diameter nozzle was operated at a frequency of 140 Hz and an electrode voltage of 750 V was used during the experiments. The working pressure is set as a function of the viscosity of the encapsulation feed (mixture of coating and active ingredient). To achieve homogeneity of the encapsulation feed and improve the adhesion of the phenolic compounds to the coating(s), the mixture was continuously stirred for 24 hours prior to encapsulation. The prolonged mixing also served to remove air bubbles that could interfere with the encapsulation process. Ionic gelation was performed dropwise in 300 mL of crosslinking solution (0.25 M $CaCl_2$), which facilitated the formation of hydrogel microbeads. The hydrogel microbeads were then mixed gently mixed in the crosslinking solution for 10 min to ensure complete solidification. The hydrogel microbeads were then washed twice with 200 ml of distilled water to remove residual non-crosslinked calcium ions adhering to the hydrogel surface.

CH as a secondary coating was added using 2 different techniques to prepare hydrogel microbeads. In the first technique, CH was dispersed in a $CaCl_2$ solution 24 hours before encapsulation to ensure complete dissolution. CH and 0.25 M $CaCl_2$ were dissolved in a 1% glacial acetic acid solution at the concentrations shown in Table 1. Another procedure consisted of preparing an alginate hydrogel microbeads that was immediately immersed in various CH solutions (Table 1)

Preprints (www.preprints.org) | NOT PEER-REVIEWED | Posted: 19 October 2023 doi:10.20944/preprints202310.1205.v1

after solidification in a $CaCl_2$ solution for 10 minutes. These hydrogel microbeads were mixed in the appropriate CH solutions for 10 min and then washed twice with 200 mL distilled water. The CH solutions were prepared 24 hours before encapsulation with 1% glacial acetic acid solution to ensure complete dissolution.

4.6. Encapsulation Efficiency Determination

After completion of hydrogel preparation, the encapsulation efficiency (*EE*, %) was calculated from the TPC released into the crosslinking solution and washed off the surface of the hydrogels and the initial TPC in the CSE used for encapsulation according to the following Equation (1):

$$EE\ (\%) = \frac{C_E - C_W}{C_E} \cdot 100 \quad (1)$$

where C_E is the initial TPC (mg), measured in the supernatant of the phenol-rich supernatant prepared for encapsulation and C_W is the TPC (mg) found in the combined calcium chloride and wash water as well as chitosan when used. The results obtained are given as the mean of replicates ± SD.

4.7. Hydrogel Drying Methods

Hydrogel microbeads prepared by ionic gelation are unstable and susceptible to contamination and spoilage due to high water content. For this purpose, the drying of hydrogels has been carried out by the following three methods:

1. Air drying—the hydrogels were placed on glass Petri dish so they did not touch, and dried at room temperature for 24 hours;
2. Vacuum drying—the hydrogels were placed in Petri dishes, places so they did not touch, and dried in preheated vacuum dryer (WOV-30, Witeg, Wertheim, Germany) at 50 °C under pressure of 300 mbar for 5 to 8 hours, depending on sample;
3. Freeze-drying—the hydrogel microbeads previously frozen at -80 °C (SWUF Ultra Low Temperature Smart Freezer, Witeg, Wertheim, Germany) were dried in freeze-drier (Freeze-dryer Alpha 2-4 LSCplus, Christ, Osterode am Harz, Germany) at -83 °C under a vacuum 0.250 mbar for 24–72 hour, depending on sample.

4.8. Characterization of Hydrogels and Dried Microbeads

4.8.1. Determination of Geometric Characteristics

Computer image analysis was used to investigate the geometric characteristics of size and shape for both hydrogels and dried microbeads. The EPSON V500 Photo Scanner (Epson America Inc., Long Beach, CA, USA), operating at 800 dpi resolution and 24-bit color depth in the sRGB model, was used to capture and digitize samples in TIFF format. Each set of experiments consisted of exactly 10 hydrogels or dry microbeads carefully arranged on a glass Petri dish to avoid contact. The Petri dish containing the samples was then placed in a dark chamber to exclude external light and minimize scanning errors. After scanning, the acquired images were thoroughly postprocessed using the ImageJ program (version 1.59g, Wayne Rasband, NIMH, Bethesda, MD, USA). The observed parameters were divided into two groups: size-related parameters included area, perimeter, and maximum and minimum Feret diameters, while shape-related parameters included circularity, roundness, and solidity. To ensure accurate measurement, the results obtained for the size parameters of the samples were converted from pixel units to millimeters, considering the known values of the resolution of the scanner´ in dpi units. Shape parameters were calculated using ImageJ User Guide-IJ 1.46r software [55]. All measurements were performed in triplicate and are given as mean values of the measurements ± SD.

Preprints (www.preprints.org) | NOT PEER-REVIEWED | Posted: 19 October 2023 doi:10.20944/preprints202310.1205.v1

4.8.2. Scanning Electron Microscopy (SEM)

The morphology of dried microbeads was examined using scanning electron microscopy (Hitachi S4700, Hitachi Scientific Ltd., Tokyo, Japan) at 10 kV. Prior to imaging, a thin gold-palladium film was applied to the dry microbeads using a sputter coater (Bio-Rad SC 502, VG Microtech, Uckfield, UK).

4.8.3. Texture Determination

The texture profile of hydrogels was evaluated using the TA.XTplus Texture Analyzer (Stable Microsystems Ltd., Surrey, UK). Each individual hydrogel underwent a dual compression cycle of 50%, with a 2-second interval between compressions and a test speed of 0.5 mm/s. An aluminum cylinder probe with a diameter of 10 mm was used for this purpose. The hardness value derived from the texture profile analysis curves, was determined after a 2-second compression when the hydrogel was compressed to 1 mm. A similar procedure was used for the dried microbeads, using the same probe to perform compression with a load of 20% at a test speed of 0.1 mm/s and determining the hardness at the maximum peak height. The texture profile of ten individual hydrogels and dried microbeads of each sample was evaluated and the hardness was reported as the mean of the measurements ± SD.

4.9. Release Study of Encapsulated Phenolic Compounds

The in vitro release of total phenolic compounds from the air, vacuum, and freeze-dried microbeads was conducted following the INFOGEST protocol [56], with some modifications. The release study included oral phase (OP), gastric phase (GP), and intestinal phase (IP), simulating the conditions of the human gastrointestinal tract. Electrolyte solutions mimicking these phases were utilized, and the process was enzyme-free. Throughout the entire 243-minute experiment, the temperature was maintained at 37 °C, and stirring was carried out using a magnetic stirrer.

To initiate the OP, 100 mg of microbeads were combined with 4 mL of simulated salivary fluid (SSF) and 25 µL of $CaCl_2(H_2O)_2$. The pH was adjusted to 7, and redistilled water was added to reach a total volume of 10 mL. After a 3-minute OP, 2 mL of the sample was removed and used for TPC determination, while 2 mL of the SSF was reintroduced into the system. After OP_3 (the index represents the total digestion time in minutes), the GP initiated by adding 8 mL of simulated gastric fluid (SGF) and 5 µL of $CaCl_2(H_2O)_2$ to the system. The pH was adjusted to 3 with 1 M HCl. Redistilled water was added to a final volume of 20 mL, and this phase lasted 120 minutes. At specific time intervals (GP_{63}, GP_{123}), 2 mL of the sample was removed and an equal volume of SGF was added back, corresponding to the approach used in OP. Finally, the intestinal phase (IP) was initiated by adding 16 mL of simulated intestinal fluid (SIF) and 40 µL of $CaCl_2(H_2O)_2$. The pH was adjusted to 7, and redistilled water was added to bring the total volume to 40 mL. This phase also lasted 120 minutes, and the sampling and recovery of the same amount of SIF at one time interval of the phase (IP_{183}) was consistent with the previous OP and GP, while at IP_{243} only sampling was conducted.

4.10. Statistical Analysis

To test the significance level of the difference between the arithmetic means of the samples representing the population, a one-way analysis of variance (ANOVA) was performed using TIBCO Statistica software (TIBCO Software Inc., Palo Alto, CA, USA). After determining statistically significant differences, an additional post-hoc test (Duncan´s test for multiple ranges) was performed to determine specific populations that showed significant differences ($p < 0.05$). Samples belonging to the same population were marked with the same letter of the alphabet in the figures or tables.

Supplementary Materials: The following supporting information can be downloaded at the website of this paper posted on Preprints.org, Figure S1. SEM image of the grape pomace extract encapsulated in air-dried (AD), vacuum-dried (VD), and freeze-dried (FD) microbeads prepared using various coatings (SA—sodium alginate, and combinations of sodium alginate with maltodextrin (dextrose equivalent 4–7)—SA+MDl, maltodextrin (dextrose equivalent 16.5–19.5)—SA+MDh, gum Arabica—SA+GA, gelatin—SA+GEL; with chitosan (CH)

dispersed in crosslinking solution at various concentrations: SA/1.5CH—1.5% (w/v), SA/1.0CH—1.0% (w/v), SA/0.5CH—0.5% (w/v); and with CH when alginate hydrogels were immersed in CH solution (image of freeze dried microbeads presented in manuscript) of various concentrations: SA(1.5CH)—1.5% (w/v), SA(1.0CH)—1.0% (w/v), SA(0.5CH)—0.5% (w/v); Figure S2. Cumulative release of total phenolic compounds (TPC) from air-dried, vacuum-dried, and freeze-dried microbeads (MB) containing grape pomace extract and coated with sodium alginate (SA) (OP-oral phase, GP-gastric phase, IP-intestinal phase, index number—duration of digestion in vitro); Figure S3. Cumulative release of total phenolic compounds (TPC) from air-dried, vacuum-dried, and freeze-dried microbeads (MB) containing grape pomace extract and coated with sodium alginate (SA) combined with (A) maltodextrin DE 4–7 (SA+MDl); (B) maltodextrin DE 16.5-19.5 (SA+MDh); (C) gum Tragacanth (SA+GT), (D) gum Arabica (SA+GA); (E) gelatin (SA+GEL) (OP-oral phase, GP-gastric phase, IP-intestinal phase, index number—duration of digestion in vitro); Figure S4. Cumulative release of total phenolic compounds (TPC) from air-dried, vacuum-dried, and freeze-dried microbeads (MB) containing grape pomace extract and coated with sodium alginate (SA) combined with chitosan dispersed in crosslinking solution in various concentrations: (A) 1.5% (SA/1.5CH); (B) 1.0% (SA/1.0CH); and (C) 0.5% (SA/0.5CH) (OP-oral phase, GP-gastric phase, IP-intestinal phase, index number—duration of digestion in vitro); Figure S5. Cumulative release of total phenolic compounds (TPC) from air-dried, vacuum-dried, and freeze-dried microbeads (MB) containing grape pomace extract and coated with sodium alginate (SA) and subsequently immersed in chitosan (CH) in various concentrations: (A) 1.5% (SA(1.5CH)); (B) 1.0% (SA(1.0CH)); and (C) 0.5% (SA/(0.5CH)), (OP-oral phase, GP-gastric phase, IP-intestinal phase, index number—duration of digestion in vitro). Table S1. Area of hydrogel microbeads and dried microbeads.; Table S2. Perimeter of hydrogel microbeads and dried microbeads; Table S3. $Feret_{MAX}$ of hydrogel microbeads and dried microbeads; Table S4: $Feret_{MIN}$ of hydrogel microbeads and dried microbeads; Table S5. Circularity of hydrogel microbeads and dried microbeads; Table S6. Roundness of hydrogel microbeads and dried microbeads; Table S7. Solidity of hydrogel microbeads and dried microbeads; Table S8. Hardness of hydrogel microbeads and dried microbeads.

Author Contributions: Conceptualization, J.M. and A.B.-K.; investigation, J.M., J.L., M.J. and R.A.; formal analysis, G.Š. and G.P.; writing—original draft preparation, J.M.; data curation, J.M., J.L., M.J. and M.P.; writing—review and editing, M.P., R.A. and A.B.-K.; supervision, A.B.-K. All authors have read and agreed to the published version of the manuscript.

Funding: This research was funded by the CROATIAN SCIENCE FOUNDATION, grant number: IP-2018-01-1227 (“Development of a sustainable integrated process for the production of bioactive isolates from food industry residues”, POPI-WinCEco); BILATERAL PROJECT CROATIA–HUNGARY, grant number: HR-HUN_2020_011 and 2019-2.1.11-TÉT-2020-00146 (″Encapsulation of polyphenol-rich extracts from food industry residues and characterization of encapsulated particles″); and by the MINISTRY OF HUMAN CAPACITIES, HUNGARY, grant number: TKP2021-EGA-32.

Institutional Review Board Statement: Not applicable.

Informed Consent Statement: Not applicable.

Data Availability Statement: Not applicable.

Acknowledgments: The authors thank the winery of the company Erdutski vinogradi d.o.o., Croatia, for the donation of grape pomace samples.

Conflicts of Interest: The authors declare no conflict of interest.

References

1. Zabot, G.L.; Schaefer Rodrigues, F.; Polano Ody, L.; Vinícius Tres, M.; Herrera, E.; Palacin, H.; Córdova-Ramos, J.S.; Best, I.; Olivera-Montenegro, L. Encapsulation of Bioactive Compounds for Food and Agricultural Applications. *Polymers* **2022**, *14*, 4194, doi:10.3390/polym14194194.
2. Antonić, B.; Jančíková, S.; Dordević, D.; Tremlová, B. Grape Pomace Valorization: A Systematic Review and Meta-Analysis. *Foods* **2020**, *9*, 1627, doi:10.3390/foods9111627.
3. Ćorković, I.; Pichler, A.; Šimunović, J.; Kopjar, M. Hydrogels: Characteristics and Application as Delivery Systems of Phenolic and Aroma Compounds. *Foods* **2021**, *10*, 1252, doi:10.3390/foods10061252.
4. Ta, L.P.; Bujna, E.; Antal, O.; Ladányi, M.; Juhász, R.; Szécsi, A.; Kun, S.; Sudheer, S.; Gupta, V.K.; Nguyen, Q.D. Effects of Various Polysaccharides (Alginate, Carrageenan, Gums, Chitosan) and Their Combination with Prebiotic Saccharides (Resistant Starch, Lactosucrose, Lactulose) on the Encapsulation of Probiotic Bacteria *Lactobacillus Casei* 01 Strain. *Int. J. Biol. Macromol.* **2021**, *183*, 1136–1144, doi:10.1016/j.ijbiomac.2021.04.170.

5. Wang, P.; Luo, Z.; Xiao, Z. Preparation, Physicochemical Characterization and In Vitro Release Behavior of Resveratrol-Loaded Oxidized Gellan Gum/Resistant Starch Hydrogel Beads. *Carbohydr. Polym.* **2021**, *260*, 117794, doi:10.1016/j.carbpol.2021.117794.
6. Sahoo, D.R.; Biswal, T. Alginate and Its Application to Tissue Engineering. *SN Appl. Sci.* **2021**, *3*, 30, doi:10.1007/s42452-020-04096-w.
7. Qin, Y. Alginate Fibres: An Overview of the Production Processes and Applications in Wound Management. *Polym. Int.* **2008**, *57*, 171–180, doi:10.1002/pi.2296.
8. Gong, Y.; Han, G.T.; Zhang, Y.M.; Zhang, J.F.; Jiang, W.; Tao, X.W.; Gao, S.C. Preparation of Alginate Membrane for Tissue Engineering. *J. Polym. Eng.* **2016**, *36*, 363–370, doi:10.1515/polyeng-2015-0065.
9. Kurowiak, J.; Kaczmarek-Pawelska, A.; Mackiewicz, A.G.; Bedzinski, R. Analysis of the Degradation Process of Alginate-Based Hydrogels in Artificial Urine for Use as a Bioresorbable Material in the Treatment of Urethral Injuries. *Processes* **2020**, *8*, 304, doi:10.3390/pr8030304.
10. Stoll, L.; Costa, T.M.H.; Jablonski, A.; Flôres, S.H.; De Oliveira Rios, A. Microencapsulation of Anthocyanins with Different Wall Materials and Its Application in Active Biodegradable Films. *Food Bioprocess. Technol.* **2016**, *9*, 172–181, doi:10.1007/s11947-015-1610-0.
11. Pudziuvelyte, L.; Marksa, M.; Sosnowska, K.; Winnicka, K.; Morkuniene, R.; Bernatoniene, J. Freeze-Drying Technique for Microencapsulation of Elsholtzia Ciliata Ethanolic Extract Using Different Coating Materials. *Molecules* **2020**, *25*, 2237, doi:10.3390/molecules25092237.
12. Tonon, R.V.; Brabet, C.; Pallet, D.; Brat, P.; Hubinger, M.D. Physicochemical and Morphological Characterisation of Açai (*Euterpe Oleraceae* Mart.) Powder Produced with Different Carrier Agents. *Int. J. Food Sci. Technol.* **2009**, *44*, 1950–1958, doi:10.1111/j.1365-2621.2009.02012.x.
13. Riseh, R.S.; Tamanadar, E.; Pour, M.M.; Thakur, V.K. Novel Approaches for Encapsulation of Plant Probiotic Bacteria with Sustainable Polymer Gums: Application in the Management of Pests and Diseases. *Adv. Polym. Technol.* **2022**, *2022*, 1–10, doi:10.1155/2022/4419409.
14. Böger, B.R.; Georgetti, S.R.; Kurozawa, L.E. Microencapsulation of Grape Seed Oil by Spray Drying. *Food Sci. Technol.* **2018**, *38*, 263–270, doi:10.1590/fst.04417.
15. Zuanon, L.A.C.; Malacrida, C.R.; Telis, V.R.N. Production of Turmeric Oleoresin Microcapsules by Complex Coacervation with Gelatin–Gum A Rabic. *J. Food Process Eng.* **2013**, *36*, 364–373, doi:10.1111/jfpe.12003.
16. Rigon, R.T.; Zapata Noreña, C.P. Microencapsulation by Spray-Drying of Bioactive Compounds Extracted from Blackberry (*Rubus Fruticosus*). *J. Food Sci. Technol.* **2016**, *53*, 1515–1524, doi:10.1007/s13197-015-2111-x.
17. Estevinho, B.N.; Damas, A.M.; Martins, P.; Rocha, F. Microencapsulation of β-Galactosidase with Different Biopolymers by a Spray-Drying Process. *Food Res. Int.* **2014**, *64*, 134–140, doi:10.1016/j.foodres.2014.05.057.
18. Sharifi, S.; Rezazad-Bari, M.; Alizadeh, M.; Almasi, H.; Amiri, S. Use of Whey Protein Isolate and Gum Arabic for the Co-Encapsulation of Probiotic *Lactobacillus Plantarum* and Phytosterols by Complex Coacervation: Enhanced Viability of Probiotic in Iranian White Cheese. *Food Hydrocoll.* **2021**, *113*, 106496, doi:10.1016/j.foodhyd.2020.106496.
19. Balaghi, S.; Mohammadifar, M.A.; Zargaraan, A. Physicochemical and Rheological Characterization of Gum Tragacanth Exudates from Six Species of Iranian *Astragalus*. *Food Biophys.* **2010**, *5*, 59–71, doi:10.1007/s11483-009-9144-5.
20. Yoon, H.J.; Shin, S.R.; Cha, J.M.; Lee, S.-H.; Kim, J.-H.; Do, J.T.; Song, H.; Bae, H. Cold Water Fish Gelatin Methacryloyl Hydrogel for Tissue Engineering Application. *PLoS ONE* **2016**, *11*, e0163902, doi:10.1371/journal.pone.0163902.
21. Al-Nimry, S.; Dayah, A.A.; Hasan, I.; Daghmash, R. Cosmetic, Biomedical and Pharmaceutical Applications of Fish Gelatin/Hydrolysates. *Mar. Drugs* **2021**, *19*, 145, doi:10.3390/md19030145.
22. Raza, Z.A.; Khalil, S.; Ayub, A.; Banat, I.M. Recent Developments in Chitosan Encapsulation of Various Active Ingredients for Multifunctional Applications. *Carbohydr. Res.* **2020**, *492*, 108004, doi:10.1016/j.carres.2020.108004.
23. Vaz, J.M.; Pezzoli, D.; Chevallier, P.; Campelo, C.S.; Candiani, G.; Mantovani, D. Antibacterial Coatings Based on Chitosan for Pharmaceutical and Biomedical Applications. *Curr. Pharm. Des.* **2018**, *24*, 866–885, doi:10.2174/1381612824666180219143900.
24. Ong, S.-Y.; Wu, J.; Moochhala, S.M.; Tan, M.-H.; Lu, J. Development of a Chitosan-Based Wound Dressing with Improved Hemostatic and Antimicrobial Properties. *Biomaterials* **2008**, *29*, 4323–4332, doi:10.1016/j.biomaterials.2008.07.034.
25. Bhattarai, N.; Gunn, J.; Zhang, M. Chitosan-Based Hydrogels for Controlled, Localized Drug Delivery. *Adv. Drug Deliv. Rev.* **2010**, *62*, 83–99, doi:10.1016/j.addr.2009.07.019.
26. Ranganathan, S.; Balagangadharan, K.; Selvamurugan, N. Chitosan and Gelatin-Based Electrospun Fibers for Bone Tissue Engineering. *Int. J. Biol. Macromol.* **2019**, *133*, 354–364, doi:10.1016/j.ijbiomac.2019.04.115.
27. Laine, P.; Kylli, P.; Heinonen, M.; Jouppila, K. Storage Stability of Microencapsulated Cloudberry (*Rubus Chamaemorus*) Phenolics. *J. Agric. Food Chem.* **2008**, *56*, 11251–11261, doi:10.1021/jf801868h.

28. Apoorva, A.; Rameshbabu, A.P.; Dasgupta, S.; Dhara, S.; Padmavati, M. Novel pH-Sensitive Alginate Hydrogel Delivery System Reinforced with Gum Tragacanth for Intestinal Targeting of Nutraceuticals. *Int. J. Biol. Macromol.* **2020**, *147*, 675–687, doi:10.1016/j.ijbiomac.2020.01.027.
29. Li, Q.; Duan, M.; Hou, D.; Chen, X.; Shi, J.; Zhou, W. Fabrication and Characterization of Ca(II)-Alginate-Based Beads Combined with Different Polysaccharides as Vehicles for Delivery, Release and Storage of Tea Polyphenols. *Food Hydrocolloids* **2021**, *112*, 106274, doi:10.1016/j.foodhyd.2020.106274.
30. Dos Santos, M.A.; Grenha, A. Polysaccharide Nanoparticles for Protein and Peptide Delivery. In *Advances in Protein Chemistry and Structural Biology*; Donev, R., Ed.; Elsevier, 2015; Vol. 98, pp. 223–261 ISBN 978-0-12-802828-5.
31. Mateus, N.; Carvalho, E.; Luís, C.; De Freitas, V. Influence of the Tannin Structure on the Disruption Effect of Carbohydrates on Protein–Tannin Aggregates. *Anal. Chim. Acta* **2004**, *513*, 135–140, doi:10.1016/j.aca.2003.08.072.
32. Shahidi, F.; Dissanayaka, C.S. Phenolic-Protein Interactions: Insight from in-Silico Analyses—a Review. *Food Prod. Process. Nutr.* **2023**, *5*, 2, doi:10.1186/s43014-022-00121-0.
33. Moschona, A.; Liakopoulou-Kyriakides, M. Encapsulation of Biological Active Phenolic Compounds Extracted from Wine Wastes in Alginate-Chitosan Microbeads. *J. Microencapsul.* **2018**, *35*, 229–240, doi:10.1080/02652048.2018.1462415.
34. Xing, N.; Li, Y.K.; Li, M.S.; Tian, F. Insight into Effects of Different Drying Methods on Morphological Properties of Sodium Alginate-Chitosan Double Coacervation Hydrogel Beads. *Appl. Mech. Mater.* **2012**, *184–185*, 1025–1029, doi:10.4028/www.scientific.net/AMM.184-185.1025.
35. Bušić, A.; Belščak-Cvitanović, A.; Vojvodić Cebin, A.; Karlović, S.; Kovač, V.; Špoljarić, I.; Mršić, G.; Komes, D. Structuring New Alginate Network Aimed for Delivery of Dandelion (*Taraxacum Officinale* L.) Polyphenols Using Ionic Gelation and New Filler Materials. *Food Res. Int.* **2018**, *111*, 244–255, doi:10.1016/j.foodres.2018.05.034.
36. Lin, C.-C.; Metters, A.T. Hydrogels in Controlled Release Formulations: Network Design and Mathematical Modeling. *Adv. Drug Deliv. Rev.* **2006**, *58*, 1379–1408, doi:10.1016/j.addr.2006.09.004.
37. Abdin, M.; Salama, M.A.; Riaz, A.; Akhtar, H.M.S.; Elsanat, S.Y. Enhanced the Entrapment and Controlled Release of *Syzygium Cumini* Seeds Polyphenols by Modifying the Surface and Internal Organization of Alginate-based Microcapsules. *J. Food Process. Preserv.* **2021**, *45*, e15100, doi:10.1111/jfpp.15100.
38. Guzman-Villanueva, D.; El-Sherbiny, I.M.; Herrera-Ruiz, D.; Smyth, H.D.C. Design and In Vitro Evaluation of a New Nano-Microparticulate System for Enhanced Aqueous-Phase Solubility of Curcumin. *Biomed. Res. Int.* **2013**, *2013*, 1–9, doi:10.1155/2013/724763.
39. Parikh, D.M. Vacuum Drying: Basics and Application. *Chem. Eng.* **2015**, *122*, 48–54.
40. Essifi, K.; Brahmi, M.; Berraaouan, D.; Ed-Daoui, A.; El Bachiri, A.; Fauconnier, M.-L.; Tahani, A. Influence of Sodium Alginate Concentration on Microcapsules Properties Foreseeing the Protection and Controlled Release of Bioactive Substances. *J. Chem.* **2021**, *2021*, 1–13, doi:10.1155/2021/5531479.
41. Devi, N.; Kakati, D.K. Smart Porous Microparticles Based on Gelatin/Sodium Alginate Polyelectrolyte Complex. *J. Food Eng.* **2013**, *117*, 193–204, doi:10.1016/j.jfoodeng.2013.02.018.
42. Nayak, A.K.; Pal, D. Development of pH-Sensitive Tamarind Seed Polysaccharide–Alginate Composite Beads for Controlled Diclofenac Sodium Delivery Using Response Surface Methodology. *Int. J. Biol. Macromol.* **2011**, *49*, 784–793, doi:10.1016/j.ijbiomac.2011.07.013.
43. Tsai, F.-H.; Kitamura, Y.; Kokawa, M. Effect of Gum Arabic-Modified Alginate on Physicochemical Properties, Release Kinetics, and Storage Stability of Liquid-Core Hydrogel Beads. *Carbohydr. Polym.* **2017**, *174*, 1069–1077, doi:10.1016/j.carbpol.2017.07.031.
44. Dai, Y.; Li, P.; Zhang, J.; Wang, A.; Wei, Q. Swelling Characteristics and Drug Delivery Properties of Nifedipine-loaded pH Sensitive Alginate–Chitosan Hydrogel Beads. *J. Biomed. Mater. Res.* **2008**, *86B*, 493–500, doi:10.1002/jbm.b.31046.
45. Siripatrawan, U.; Vitchayakitti, W. Improving Functional Properties of Chitosan Films as Active Food Packaging by Incorporating with Propolis. *Food Hydrocoll.* **2016**, *61*, 695–702, doi:10.1016/j.foodhyd.2016.06.001.
46. Kurozawa, L.E.; Hubinger, M.D. Hydrophilic Food Compounds Encapsulation by Ionic Gelation. *Curr. Opin. Food Sci.* **2017**, *15*, 50–55, doi:10.1016/j.cofs.2017.06.004.
47. Deladino, L.; Anbinder, P.S.; Navarro, A.S.; Martino, M.N. Encapsulation of Natural Antioxidants Extracted from *Ilex Paraguariensis*. *Carbohydr. Polym.* **2008**, *71*, 126–134, doi:10.1016/j.carbpol.2007.05.030.
48. Anbinder, P.S.; Deladino, L.; Navarro, A.S.; Amalvy, J.I.; Martino, M.N. Yerba Mate Extract Encapsulation with Alginate and Chitosan Systems: Interactions between Active Compound Encapsulation Polymers. *J. Encapsulation Adsorpt. Sci.* **2011**, *1*, 80–87, doi:10.4236/jeas.2011.14011.
49. Belščak-Cvitanović, A.; Komes, D.; Karlović, S.; Djaković, S.; Špoljarić, I.; Mršić, G.; Ježek, D. Improving the Controlled Delivery Formulations of Caffeine in Alginate Hydrogel Beads Combined with Pectin, Carrageenan, Chitosan and Psyllium. *Food Chem.* **2015**, *167*, 378–386, doi:10.1016/j.foodchem.2014.07.011.

50. Belščak-Cvitanović, A.; Đorđević, V.; Karlović, S.; Pavlović, V.; Komes, D.; Ježek, D.; Bugarski, B.; Nedović, V. Protein-Reinforced and Chitosan-Pectin Coated Alginate Microparticles for Delivery of Flavan-3-Ol Antioxidants and Caffeine from Green Tea Extract. *Food Hydrocoll.* **2015**, *51*, 361–374, doi:10.1016/j.foodhyd.2015.05.039.
51. Antigo, J.L.D.; Bergamasco, R.D.C.; Madrona, G.S. Effect of Ph on the Stability of Red Beet Extract (Beta Vulgaris l.) Microcapsules Produced by Spray Drying or Freeze Drying. *Food Sci. Technol.* **2017**, *38*, 72–77, doi:10.1590/1678-457x.34316.
52. Martinović, J.; Lukinac, J.; Jukić, M.; Ambrus, R.; Planinić, M.; Šelo, G.; Klarić, A.-M.; Perković, G.; Bucić-Kojić, A. Physicochemical Characterization and Evaluation of Gastrointestinal In Vitro Behavior of Alginate-Based Microbeads with Encapsulated Grape Pomace Extracts. *Pharmaceutics* **2023**, *15*, 980, doi:10.3390/pharmaceutics15030980.
53. Martinović, J.; Lukinac, J.; Jukić, M.; Ambrus, R.; Planinić, M.; Šelo, G.; Klarić, A.-M.; Perković, G.; Bucić-Kojić, A. In Vitro Bioaccessibility Assessment of Phenolic Compounds from Encapsulated Grape Pomace Extract by Ionic Gelation. *Molecules* **2023**, *28*, 5285, doi:10.3390/molecules28135285.
54. Waterhouse, A.L. Determination of Total Phenolics. In *Current Protocols in Food Analytical Chemistry*; Wrolstad, R.E., Ed.; John Wiley & Sons Inc.: New York, NY, USA, 2001; p. I1.1.1-I1.1.8.
55. ImageJ User Guide IJ 1.46r. Available online: https://imagej.nih.gov/ij/docs/guide/146.html (accessed on 10 January 2023).
56. Brodkorb, A.; Egger, L.; Alminger, M.; Alvito, P.; Assunção, R.; Ballance, S.; Bohn, T.; Bourlieu-Lacanal, C.; Boutrou, R.; Carrière, F.; Clemente, A.; Corredig, M.; Dupont, D.; Dufour, C.; Edwards, C.; Golding, M.; Karakaya, S.; Kirkhus, B.; Le Feunteun, S.; Lesmes, U.; Macierzanka, A.; Mackie, A. R.; Martins, C.; Marze, S.; McClements, D. J.; Ménard, O.; Minekus, M.; Portmann, R.; Santos, C. N.; Souchon, I.; Singh, R. P.; Vegarud, G. E.; Wickham, M. S. J.; Weitschies, W.; Recio, I. INFOGEST Static In Vitro Simulation of Gastrointestinal Food Digestion. *Nat. Protoc.* **2019**, *14*, 991–1014, doi:10.1038/s41596-018-0119-1.